

RESEARCH ARTICLE

Allosteric differences dictate GroEL complementation of *E. coli*

Jared Sivinski¹  | Duc Ngo¹ | Christopher J. Zerio¹ | Andrew J. Ambrose¹ | Edmond R. Watson² | Lynn K. Kaneko¹ | Marius M. Kostelic³ | Mckayla Stevens⁴ | Anne-Marie Ray⁴ | Yangshin Park^{4,5,6} | Chunxiang Wu⁷ | Michael T. Marty³ | Quyen Q. Hoang^{4,5,6} | Donna D. Zhang¹ | Gabriel C. Lander² | Steven M. Johnson⁴  | Eli Chapman¹

¹Department of Pharmacology and Toxicology, College of Pharmacy, The University of Arizona, Tucson, Arizona, USA

²Department of Integrative Structural and Computational Biology, Scripps Research, La Jolla, California, USA

³Department of Chemistry and Biochemistry, The University of Arizona, Tucson, Arizona, USA

⁴Department of Biochemistry and Molecular Biology, Indiana University School of Medicine, Indianapolis, Indiana, USA

⁵Stark Neurosciences Research Institute, Indiana University School of Medicine, Indianapolis, Indiana, USA

⁶Department of Neurology, Indiana University School of Medicine, Indianapolis, Indiana, USA

⁷Department of Molecular Biophysics and Biochemistry, Yale University, New Haven, Connecticut, USA

Correspondence

Eli Chapman, Department of Pharmacology and Toxicology, College of Pharmacy, The University of Arizona, 1703 E. Mabel St., PO Box 210207, Tucson, AZ 85721, USA.
 Email: chapman@pharmacy.arizona.edu

Funding information

Research reported in this publication was supported by the National Institute of General Medical Sciences (NIGMS) of the National Institutes of Health (NIH) under Award no. R01GM120350. S.M.J., Q.Q.H., and E.C. Q.Q.H. additionally acknowledge support by NIH grants 5R01GM111639 and 5R01GM115844. M.T.M. and M.M.K. were supported by NIH R35GM128624. J.S., C.J.Z., and M.M.K. are supported by NIH T32 GM008804. The content is solely the responsibility of the authors and does not necessarily represent the official views of the NIH

Abstract

GroES/GroEL is the only bacterial chaperone essential under all conditions, making it a potential antibiotic target. Rationally targeting ESKAPE GroES/GroEL as an antibiotic strategy necessitates studying their structure and function. Herein, we outline the structural similarities between *Escherichia coli* and ESKAPE GroES/GroEL and identify significant differences in intra- and inter-ring cooperativity, required in the refolding cycle of client polypeptides. Previously, we observed that one-half of ESKAPE GroES/GroEL family members could not support cell viability when each was individually expressed in GroES/GroEL-deficient *E. coli* cells. Cell viability was found to be dependent on the allosteric compatibility between ESKAPE and *E. coli* subunits within mixed (*E. coli* and ESKAPE) tetradecameric GroEL complexes. Interestingly, differences in allostery did not necessarily result in differences in refolding rate for a given homotetradecameric chaperonin. Characterization of ESKAPE GroEL allostery, ATPase, and refolding rates in this study will serve to inform future studies focused on inhibitor design and mechanism of action studies.

Abbreviations: ADP, adenosine diphosphate; ATP, adenosine triphosphate; CD-MS, charge detection-mass spectrometry; dMDH, denatured malate dehydrogenase; EM, electron microscopy; ESKAPE, *Enterococcus faecium*, *Staphylococcus aureus*, *Klebsiella pneumoniae*, *Acinetobacter baumannii*, *Pseudomonas aeruginosa*, *Enterobacter* species; KNF, Koshland-Nemethy-Filmer; MDH, malate dehydrogenase; MS, mass spectrometry; MWC, Monod-Wyman-Changeux; SEC-MALS, size-exclusion chromatography coupled with multi-angle light scattering; SR1, single ring mutant of GroEL.

KEYWORDS

allostery, chaperone, chaperonin, ESKAPE, GroEL, GroES

1 | INTRODUCTION

ESKAPE pathogens (*Enterococcus faecium*, *Staphylococcus aureus*, *Klebsiella pneumoniae*, *Acinetobacter baumannii*, *Pseudomonas aeruginosa*, and *Enterobacter cloacae*) are a major contributor to hospital-acquired antibiotic-resistant infections and result in significant morbidity and mortality. With only one drug brought to market with a unique mechanism of action to target these pathogens within the last 20 years, the basis for this study is to characterize a proposed novel target within these organisms.^{1,2} GroEL, a 57 kDa protein that assembles into an 800 kDa homo-tetradecamer, along with its homoheptameric 70 kDa cochaperone GroES, assists in the refolding of hundreds of proteins in *E. coli* with dozens of stringent clients (requiring GroEL, GroES, and ATP) that are essential for cell viability.^{3–7} Each GroEL subunit (monomer) is made up of apical, intermediate, and equatorial domains. The equatorial domain maintains intra-ring and inter-ring contacts and binds and hydrolyzes ATP. Hydrophobic residues lining the surface of the apical domain allow binding of client polypeptide (denatured or partially folded) with high affinity. The apical domain also interacts with GroES and undergoes large rigid body movements that create the hydrophilic chamber for clients to refold away from biomolecules in the crowded cellular environment. The intermediate domain connects the apical and equatorial domains and allows allosteric transmission of a signal between and within GroEL rings.^{8–11} Real-time genetic experiments in *E. coli* have shown that suppression of GroES/GroEL protein expression leads to protein aggregation and is bactericidal.^{4,12} Additional studies have shown that small-molecule inhibitors of the GroEL chaperonin (large, ring-shaped chaperones are called chaperonins) function as antibiotics *in vitro*.^{13–15} Transposon studies in the ESKAPE pathogens suggest *groESL* is similarly essential in these bacteria.^{16–21} Unlike *E. coli* GroES/GroEL (GroESL^{coli}), ESKAPE GroES/GroEL (GroESL^{ESKAPE}) are not well studied. Functional replacement of GroEL^{coli} with GroEL from other organisms in *E. coli* has been reported,^{12,22} although organism rescue is not a universal trend.^{23,24} To pursue GroESL^{ESKAPE} as a potential antibiotic target in these medically relevant pathogens, we attempted to express these chaperonins in *E. coli*²⁵ for further purification and high throughput molecule screening in a biochemical assay.

In our previous work, we found that only half of the GroESL^{ESKAPE} were able to rescue GroESL deficient

LG6 *E. coli*. However, in more stringent systems, all GroESL^{ESKAPE} except for *groESL*^{*S. aureus*} was able to rescue *E. coli* without *groESL*^{coli} present.²⁵ Pull-down experiments indicated that when GroEL^{ESKAPE} was co-expressed with GroEL^{coli}, the purified GroEL tetradecamers contained monomers from both species (Figure 1). Of the GroESL^{ESKAPE} which could not rescue LG6, it was found the respective heterooligomeric GroELs were devoid of ATPase activity. We hypothesized this lack of activity to be due to differences in allostery, which could in turn disrupt the refolding cycle of GroEL and compromise cell viability. The *E. coli* GroEL refolding cycle requires ATP, client polypeptide, and GroES (Figure 2), which drive coordinated intra and inter-ring movements that facilitate client protein refolding in a two-stroke fashion.^{26–29} This critical ATP-dependent process of nested cooperativity (Figure 2A) involves positive Monod-Wyman-Changeux (MWC)-type concerted cooperativity within each GroEL heptamer as well as integrated negative Koshland-Nemethy-Filmer (KNF)-type sequential cooperativity between GroEL heptamers.^{30–34} Each GroEL ring heptamer exists in either the tense (T) or relaxed (R) state. The T state denotes low ATP affinity and high unfolded polypeptide affinity, whereas the R state denotes high affinity for ATP and low affinity for unfolded polypeptide.^{35,36} In the presence of increasing ATP concentrations, the back-to-back GroEL tetradecamer (two heptameric GroEL rings make up the tetradecamer (Figure 1)) transitions from the T-T state to the T-R and finally R-R state. The GroEL refolding cycle outlined in Figure 2B serves as a general overview of back-to-back GroEL ring regulation and is not representative of other model types that exist in the literature.^{37–40} In the presence of ATP and unfolded polypeptide (Figure 2B, step 1) as well as GroES (Figure 2B, step 2), GroES caps the GroEL cis ring in the R state and drives ejection of the unfolded polypeptide from the apical domain into the cavity. After 10 seconds, ATP bound to the cis-ring of GroEL is hydrolyzed (Figure 2B, step 3) and the cycle repeats on the opposing trans-ring after ATP, unfolded polypeptide (Figure 2B, step 4), and GroES are bound (Figure 2B, step 5).^{41,42} Trans-ring ATP binding facilitates the release of GroES, polypeptide, and nucleotide from the cis-ring (opposite) of GroEL, which promotes client refolding in the newly formed cis-ring (Figure 2B, step 6).⁴³

Herein, we report the intra-ring and inter-ring cooperativity values, inter-ring coupling free energies, V_{max} , K_m , and allosteric transition values for GroEL^{ESKAPE}. Additionally, compatible allostery can be restored by

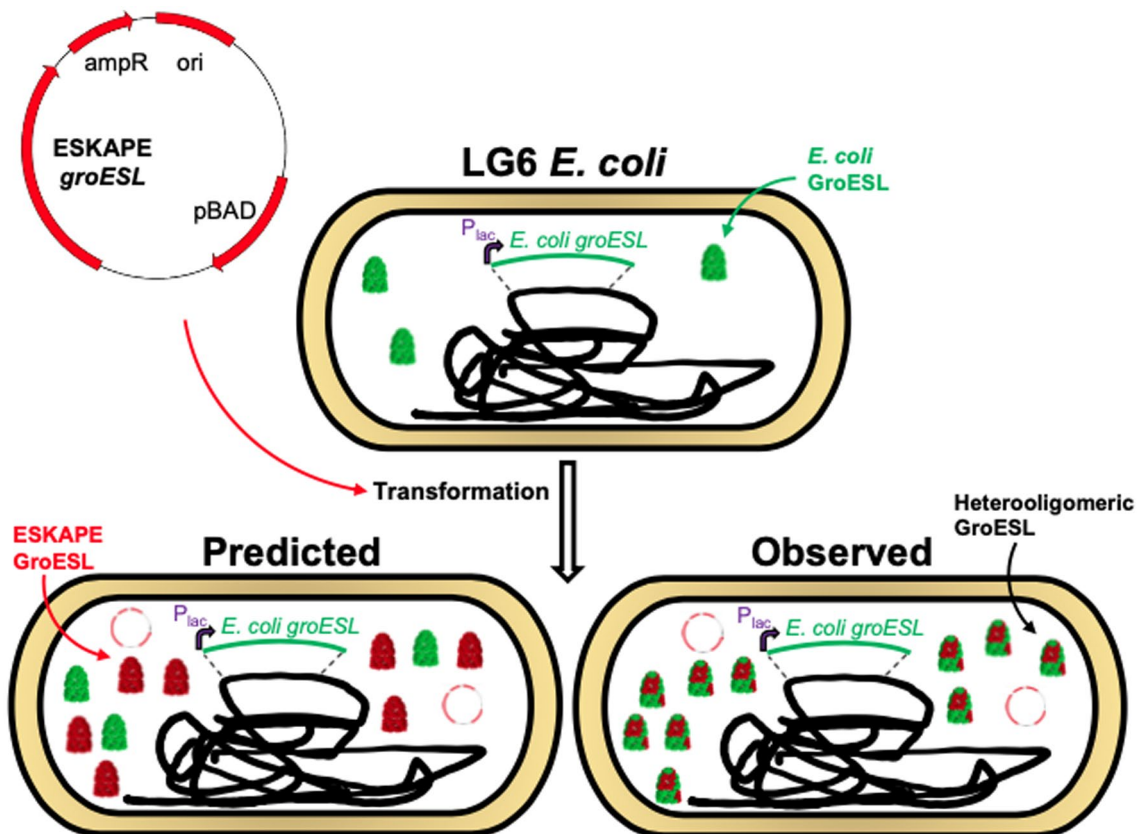


FIGURE 1 Heterooligomeric GroESL is generated during co-expression of GroESL^{coli} and GroESL^{ESKAPE}. GroESL^{ESKAPE} expressed in *lac*-promoted *groESL* LG6 *E. coli* form GroESL particles made up of GroESL^{coli} and GroESL^{ESKAPE}. Adapted from CMS Kumar, 2021, *Front Mol Biosci*.

generating chimeric monomers of GroEL that assemble into a functional tetradecamer. We also expressed and purified nonfunctional heterooligomeric GroELs which were found not to support cell viability and were devoid of ATPase activity and client refolding capabilities. This work and the previous²⁵ aim to better understand the similarities and differences of *E. coli* and ESKAPE pathogen GroES/GroEL to predict and explain inhibitor selectivity and potency as a means of setting forth a new class of antibiotics not known to have resistant variants in the wild.

2 | MATERIALS AND METHODS

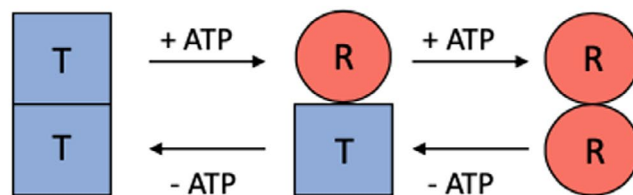
2.1 | Protein expression and purification

ESKAPE GroESL were individually expressed in MG1655 knock-in strains (containing chromosomal ESKAPE *groESL* replacing *E. coli groESL*) generated by phage lambda-derived Red recombination⁴⁴ using ESKAPE *groESL* cloned into pET21b along with pCS6 (T7 RNA polymerase helper plasmid) for overexpression and purification (single copy, chromosomal expression yields

much lower protein yields than plasmid overexpression). ESKAPE GroEL was purified similarly to *E. coli* GroEL by anion exchange chromatography, hydrophobic interaction chromatography, Affi-gel Blue resin, and sizing column chromatography.¹⁵ Into ESKAPE *groESL* knock-in MG1655 was transformed pCS6 and ESKAPE *groESL* pET21b. Overnight cultures were added to terrific broth (250–500 ml per 2L baffled flask) followed by plasmid induction at an OD₆₀₀ of 0.6 by the addition of arabinose (0.2% final concentration) to culture flasks. Expression was allowed to continue up to four hours at 37°C, after which cells were pelleted at 7200 g for 10 min at 4°C. Pellets were resuspended in 50 mM Tris pH 7.4, 50 mM KCl, 1 mM DTT, and 1 mM PMSF and homogenized using Microfluidizer LM10. The lysate was clarified by centrifugation (22 000 g for 45 min) at 4°C. Clarified lysate was loaded onto preequilibrated FFQ resin (Cytiva) and eluted using a 0 to 1M NaCl (containing 50 mM Tris pH 7.4, 1 mM DTT buffer) gradient over 10 column volumes. GroEL-containing fractions were pooled, stirred, and slowly adjusted to 1.2M ammonium sulfate at 4°C, followed by clarification at 4°C for 45 min at 22 000 g. The clarified pool was added to a preequilibrated Source 15ISO (Cytiva) and eluted over 1 column volume with

(A)

Nested Allosterity



(B)

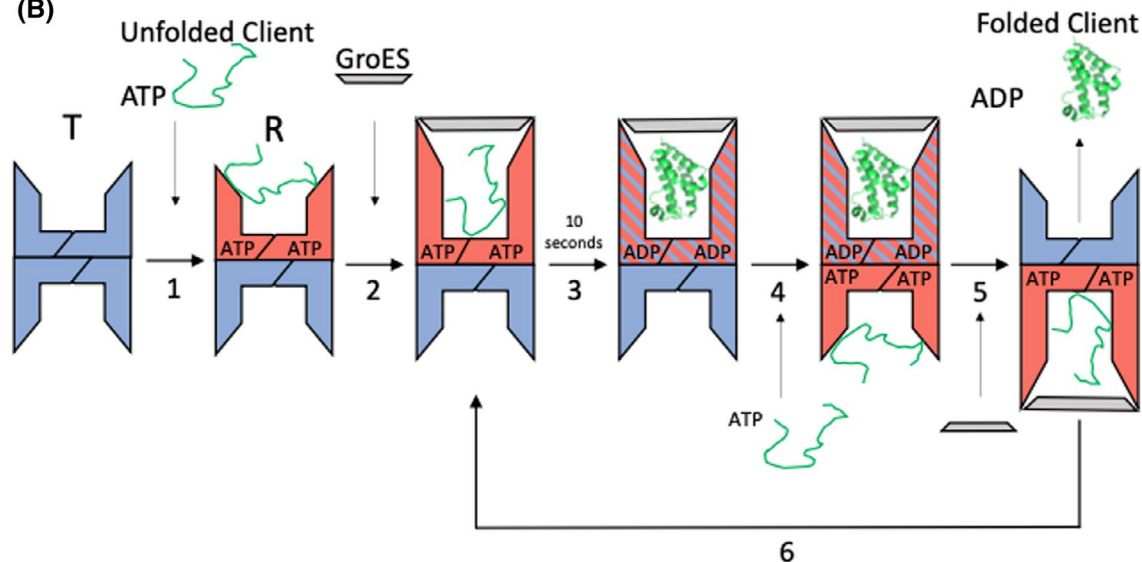


FIGURE 2 Overview of GroEL nested allosterity and general refolding cycle. (A) GroEL nested allosterity with GroEL back-to-back heptamers shown as squares (blue) in the tense state (T) with low ATP affinity and high unfolded polypeptide client affinity. GroEL heptamer shown in the relaxed (red) state (R) with high affinity for ATP and low affinity for unfolded polypeptide client. (B) GroESL refolding cycle with GroEL heptamer in the tense (blue), relaxed (red), or during the transition from relaxed to tense (blue/red stripes) states. Adapted from Clare DK, 2012, *Cell*. Folded client protein (green) shown from PDB 3S92. Steps 1 through 6 of the general refolding cycle are outlined under each arrow

50 mM Tris pH 7.4, 50 mM KCl, 150 mM NaCl, and 1 mM DTT. Pooled GroEL fractions were incubated with 1 ml of preequilibrated Affi-gel Blue resin for every 30 mg of GroEL protein and placed on a rocking platform for 48 h at 4°C. GroEL recovered from Affi-gel Blue resin was finally concentrated to a volume less than 12 ml and added to a preequilibrated Hiload 26/60 Superdex 200 sizing column (GE) and eluted in less than one column volume. GroEL fractions were analyzed by electron microscopy and fractions containing GroEL with an appropriate quaternary structure were pooled, concentrated, and frozen for future use. Purity and quaternary structure were supported by SDS-PAGE, Native-PAGE, native MS, CD-MS, size-exclusion chromatography coupled with multi-angle light scattering (SEC-MALS), and/or electron microscopy.

ESKAPE GroES was purified similarly to *E. coli* GroES by anion and cation interaction chromatography as well as sizing column chromatography.¹⁵ ESKAPE GroES

expressed as above was loaded onto preequilibrated FFQ resin (Cytiva) and eluted using a 0 to 1-M NaCl (containing 50 mM Tris pH 7.4, 1 mM DTT buffer) gradient over 10 column volumes. GroES containing fractions were pooled and adjusted to pH 4.6 using 50 mM sodium acetate pH 4.6 buffer. pH-adjusted GroES was added to a preequilibrated FFSP (Cytiva) column and eluted over 10 column volumes using a 0 to 1M NaCl (containing 50 mM Tris pH 7.4, 1 mM DTT buffer) gradient. GroES containing fractions were pooled, concentrated, and loaded onto a preequilibrated Hiload 26/600 Superdex 75 (GE) and eluted in less than one column volume. GroES fractions were analyzed by SDS-PAGE for purity, as well as Native-PAGE and/or electron microscopy (in concert with GroEL) for proper quaternary structure. Pooled fractions were concentrated and frozen for future use.

Chimeric and heterooligomeric GroEL were purified as reported previously.²⁵

2.2 | ATPase assay

The malachite green assay⁴⁵ was used to detect the presence of inorganic phosphate released during ATP hydrolysis by GroEL. Malachite green was made with final concentrations of 0.034% malachite green, 1.04% ammonium molybdate, and 1M HCl. Prior to performing assays, Tween 20 was added to a final concentration of 0.004% to the malachite green solution. Serial dilution of ATP ranges from 0.01 to 5 mM in reaction buffer (50 mM Tris pH 7.4, 50 mM KCl, 10 mM MgCl₂, 1 mM DTT) in 384-well clear plates with 10 μ l volume per well. 10 μ l of GroEL protein (150 nM) was added to consecutive wells with ATP at room temperature at varying intervals to determine the initial rates of ATP hydrolysis. Forty microliters of malachite green were added to each reaction well (total volume of each well is 60 μ l) and plates were read immediately using SpectraMax ID5 plate reader at 660 nm absorbance to determine initial ATP hydrolysis rates (Figure 4). Data were generated in at least triplicate with averages plotted using GraphPad Prism 6.0.

ESKAPE GroESL ATPase activity was measured as above with the exception of using a single concentration of ATP as noted in the text. GroES was also added in multiple noted concentrations in comparison to a single concentration of GroEL. Data were generated in at least triplicate. Figures were generated using GraphPad Prism 6.0.

2.3 | dMDH refolding assay

dMDH refolding by ESKAPE GroESL was performed as previously reported with *E. coli* GroESL.¹⁵ 5 mg/ml MDH from porcine heart (Sigma) was diluted 1:1 with denaturation solution (7M guanidine, 50 mM Tris pH 7.4, 50 mM DTT) for one to three hours at room temperature before forming binary complex (83.33 nM GroEL and 20 nM dMDH) in 50 mM Tris pH 7.4, 50 mM KCl, 10 mM MgCl₂, 1 mM DTT (final guanidine concentration is less than 1 mM and does significantly alter chaperonin function). GroES was added at the noted concentrations to the binary solutions and a volume of 30 μ l was dispensed into a clear 384-well plate (Greiner). In addition to GroES, GroEL, and dMDH solution (binary solution), three other solutions were tested to ensure proper assay behavior: (1) Native MDH only control (to measure maximum MDH activity rate) (2) dMDH only control (to measure spontaneous refolding activity) (3) GroEL and dMDH only (measures GroEL mediated refolding of dMDH without GroES cochaperone). To each of the four solutions, 20 μ l of ATP solution (in binary buffer) at a concentration of 2.5 mM was added to start the refolding process. The assay was incubated at 37°C and quenched with 10 μ l of 0.6 M

EDTA pH 8.0 at multiple timepoints (for determination of refolding kinetics). To determine the extent of dMDH refolded, 20 μ l of assay solution (50 mM Tris pH 7.4, 50 mM KCl, 1 mM DTT, 20 mM sodium mesoxalate, and 2.4 mM NADH) was added to all wells followed by monitoring absorbance values at 340 nm using a SpectraMax ID5 plate reader. Absorbance readings were taken periodically until absorbance values reached their minima. Rate determination and figure generation were done by plotting data in GraphPad Prism 6.0. All data were generated at least in triplicate.

2.4 | GroEL activity analysis

Analysis of GroEL initial, maximum velocity, and K_m were determined by fitting low ATP concentration of (<312.5 μ M) to Hill equation:

$$V_0 = V_{\max}K[S]^n/(1 + K[S]^n) \quad (1)$$

where V_0 and V_{\max} are initial and maximum ATPase velocities, $[S]$ is the concentration of substrate (ATP), K is the apparent ATP binding constant, and n is Hill coefficient. Analysis of cooperativity for GroEL species was fit into the nested cooperativity equation³³ using the entire data of ATP concentrations (0.01–5 mM). The nested cooperativity equation combined both the MWC model of cooperativity and sequential KNF-type transition (second level of allostery between the two rings of the GroEL particle), for all non-chimera analysis ($c = 0$) assuming exclusive binding. While chimera analysis ($c > 0$) estimated values of different parameters using nested cooperativity equation without fixing $V_{\max(1)}$ and $V_{\max(2)}$. Each individual species of GroEL data (0.01–5 mM) were fitted individually to the nested cooperativity equation. Figures were generated using GraphPad Prism 6.0.

$$\bar{y} = \{c\alpha(1+c\alpha)^{2N-1} + L_1c\alpha(1+c\alpha)^{N-1}(1+\alpha)^N + L_1\alpha(1+c\alpha)^N(1+\alpha)^{N-1} + L_1L_2\alpha(1+\alpha)^{2N-1}\} / \{(1+c\alpha)^{2N} + 2L_1(1+c\alpha)^N(1+\alpha)^N + L_1L_2(1+\alpha)^{2N}\}$$

$$\alpha = [S]/K_R, c = \frac{K_R}{K_T}, \text{ and } 2N = 14$$

2.5 | Size-exclusion chromatography coupled with multi-angle light scattering

To determine the absolute molecular weight of the protein complexes in solution, we used multiple-angle light scattering. The experimental setup includes an AKTA purifier FPLC (GE Healthcare Biosciences, Piscataway, New

TABLE 1 Parameters fitted for ATPase activity of GroEL species using MWC model of cooperativity and sequential KNF-type transition

	Coli GroEL	EF GroEL	KP GroEL
K_m (μM)	38.57 (0.7240)	26.48 (2.275)	25.63 (2.360)
K_{cat}/K_m ($\text{M}^{-1} \text{S}^{-1}$)	1252.42 (86.64)	1893.81 (310.473)	1345.88 (222.87)
V_{max} (μM)	3.136 (0.02643)	3.243 (0.1142)	2.109 (0.08202)
L1	1.43×10^{-3} (3.634×10^{-4})	7.253×10^{-3} (2.933×10^{-3})	1.78×10^{-2} (1.9×10^{-2})
L2	7.214×10^{-9} (6.056×10^{-9})	1.221×10^{-5} (1.756×10^{-5})	5.58×10^{-6} (2.474×10^{-5})
1st transition (μM)	38.57 (0.7240)	26.48 (2.275)	25.63 (2.360)
2nd transition (μM)	1309 (1.03)	315.2 (1.134)	3033.9 (4.39)
C	0	0	0
$n(+)$	2.779 (0.1303)	2.841 (0.5697)	3.222 (0.7626)
$n(-)$	4.564 (1.003)	3.368 (1.524)	0.7418 (0.5188)
Delta G (kcal mol^{-1})	-7.23	-2.465	-4.779
LG6 Rescue?	Y	N	Y
AI90 Rescue?	Y	N	Y
Knock-In?	Y	Y	Y

Note: L1 and L2 are apparent allosteric constant ($L1 = [\text{TR}]/[\text{TT}]$) and ($L2 = [\text{RR}]/[\text{TR}]$). Presented here are calculations for K_{cat}/K_m per subunit and $n(+)$ = Hill coefficient for positive allosteric transition and $n(-)$ = Hill coefficient for negative allosteric transition, and delta G = inter-ring cooperative free energy. *E. coli* (Coli), *E. faecium* (EF), *K. pneumoniae* (KP), *A. baumannii* (AB), *P. aeruginosa* (PA), *E. cloacae* (EC). Error reported as standard error of the mean and all experiments performed at 24°C. Coupled with their respective GroES, rescue in LG6, AI90, or knock-in strains are outlined with the noted GroEL as yes (Y), no (N), or not applicable (N/A).

Jersey) with a silica-based size exclusion chromatography column (WTC-030S5, Wyatt Technology Corporation, Santa Barbara, California) as a liquid size-exclusion chromatography (SEC) unit. Downstream from the SEC is a refractive index detector (Optilab T-rEX, Wyatt Tech.) followed by a multiple light scattering detector (Dawn HeleosII, Wyatt Tech.) for determining protein concentration and particle size, respectively. Each sample injection consisted of ~0.5 mg protein mass in buffer containing 50 mM Tris-HCl pH 7.4, 150 mM NaCl, and 1 mM DTT. The flow rate was set at 0.4 ml/min and data were collected in 1-s intervals. Data processing and analysis were performed using the ASTRA software (Wyatt Tech.). Figures were generated using GraphPad Prism 6.0.

2.6 | Native mass spectrometry analysis

GroEL was first diluted to 2.5 mg/ml then buffer exchanged with 2 consecutive micro Bio-spin 6 columns (BioRad) into 0.2 M ammonium acetate (Sigma-Aldrich) to remove residual salts. Needles used for nano-electrospray ionization were pulled in house using a P-1000-micropipette puller (Sutter Instruments). Native mass spectrometry (MS) analysis was performed on a Q-Exactive HF quadrupole-Orbitrap mass spectrometer equipped with Ultra-High Mass Range (UHMR) research modifications (Thermo Fisher Scientific, Bremen). Native MS parameters for GroEL have been previously described.⁴⁶ Briefly, GroEL was analyzed with argon

as the collision gas and the gas pressure was set to 10. High m/z detector optimization and high m/z transfer optics were used. The capillary temperature was set to 200°C, and the spray voltage was set to 1100 V. The m/z range was set to 2000–25 000 m/z . Collected mass spectra were then deconvolved using UniDec to determine the intact mass.⁴⁷ For UniDec deconvolution, the charge range was set from 40 to 100 and the mass range was set from 100–1000 kDa. The m/z FWHM was set to 1, the point smooth function was set to 1, and the Beta parameter was set to 50.^{48,49}

2.7 | Charge detection-mass spectrometry analysis

Charge detection-mass spectrometry (CD-MS) instrument parameters for GroEL^{*E. faecium*} analysis match previously described parameters for GroEL.⁴⁶ Briefly, argon was used as the collisional gas, the transient time was set to 512 ms, the trapping gas setting was set between 5–7 (pressures of $7.31\text{--}8.48 \times 10^{-11}$ mbar), and the noise threshold was set to 0. Other MS parameters match the conventional native MS parameters for GroEL^{*E. faecium*} described in the previous section.

GroEL^{*E. faecium*} CD-MS data were then deconvolved with UniDecCD (UCD) to remove charge uncertainty from the data and obtain the intact mass distribution. The UCD algorithm has been previously described and is part of the UniDec open-source software package.^{46,47} Parameters for

AB GroEL	PA GroEL	EC GroEL	PA/Coli GroEL Chimera
41.95 (3.319)	70.70 (0.9603)	26.41 (1.152)	17.11 (1.361)
1257.02 (185.51)	892.13 (309.82)	1404.2 (137.68)	2987.05 (282.42)
3.384 (0.1154)	3.968 (0.03087)	2.271 (0.03880)	3.319 (0.08474)
6.389×10^{-3} (3.279×10^{-3})	1.089×10^{-4} (3.360×10^{-5})	2.316×10^{-3} (1.157×10^{-3})	6.395×10^{-2} (2.727×10^{-2})
9.676×10^{-6} (1.659×10^{-5})	3.417×10^{-8} (2.581×10^{-8})	5.839×10^{-11} (1.284×10^{-10})	6.556×10^{-6} (1.470×10^{-5})
41.95 (3.319)	70.70 (0.9603)	26.41 (1.152)	17.11 (1.361)
857.9 (1.199)	806.5 (1.203)	1438 (1.022)	728.9 (1.1624)
0	0	0	0.01
2.381 (0.3856)	3.567 (0.03087)	2.440 (0.2189)	1.633 (0.1807)
3.186 (1.451)	4.187(1.461)	6.166 (0.8095)	2.227(0.7449)
-4.685	-5.305	-12.4	-6.388
Y	N	Y	Y
Y	Y	Y	N/A
Y	Y	Y	N/A

UCD deconvolution of GroEL^{E. Faecium} include a m/z bin of 5, a charging bin of 1, Gaussian smoothing (m/z) set to 3, Gaussian smoothing (z) set to 1, centroid filtering width of 1, a m/z spread FWHM of 5, and a charge spread FWHM of 5. The smooth charge states feature was turned off due to unresolved charge states in the raw data (Figure S5A), the point smooth width was set to 5, and the m/z to mass transformation was set to interpolate.

2.8 | Negative stain electron microscopy

Electron microscopy grids were prepared as previously described.⁵⁰ Grids were treated using easiGlo (Pelco) glow discharge for 30 s at 15 mA (0.39 mbar). GroEL was prediluted (5 mg/ml, 0.5 mg/ml, 0.05 mg/ml) in Tris-buffered saline pH 7.4 and placed on grids for 60 s prior to washing/staining using the rapid flushing method. Stained grids were visualized using Leica Tecnai Spirit Transmission Electron Microscope (100 kV) up to 98 kx.

3 | RESULTS

3.1 | Purified ESKAPE GroELs have a tetradecameric structure

Based upon previous work,²⁵ expression of GroEL^{ESKAPE} in the presence of GroEL^{coli} generated heterooligomeric

chaperones (Figure 1) which supported cell viability in GroESL^{coli} deficient LG6 *E. coli* in some cases (GroEL^{coli} expression with GroEL^{K. pneumoniae}, GroEL^{A. baumannii}, or GroEL^{E. cloacae}), but not in others (GroEL^{coli} expression with GroEL^{S. aureus}, GroEL^{E. faecium}, or GroEL^{P. aeruginosa}) (Table 1). To obtain homotetradecameric GroESL^{ESKAPE} (without GroESL^{coli} contamination), we simultaneously knocked out *groESL*^{coli} from the *E. coli* chromosome and knocked in respective *groESL*^{ESKAPE} using phage lambda-derived Red recombination.⁴⁴ GroESL^{ESKAPE} was then overexpressed using an inducible plasmid (*groESL*^{ESKAPE} insert) within the respective knock-in strains for greater protein yield (compared to a single copy, chromosomal expression alone). All GroEL chaperones in this study were predicted to adopt a tertiary structure similar to GroEL^{coli} by Swiss Model (Figures S1 and S2) and AlphaFold (Figure S3). Predicted GroEL^{ESKAPE} models generated by AlphaFold were further aligned with GroEL^{coli} in PyMOL (Figure S3) to support this claim.^{51,52} We confirmed all GroEL^{ESKAPE} in this study indeed form tetradecamers by SEC-MALS, native mass spectrometry (MS), CD-MS,^{46,47} and/or cryo-EM (Figures 3, S4, and S5). Each of the chaperones formed stable tetradecamers with exception of GroEL^{E. faecium}, which was found to form a tetradecamer, but disassembled after one week at 4°C into dimers, trimers, and tetramers (Figure S4) and was also noted to have the lowest intra-ring coupling energy (Table 1). Based upon our SEC-MALS, native MS, and CD-MS data, it seems as though with GroEL^{E. faecium}, the heptameric rings

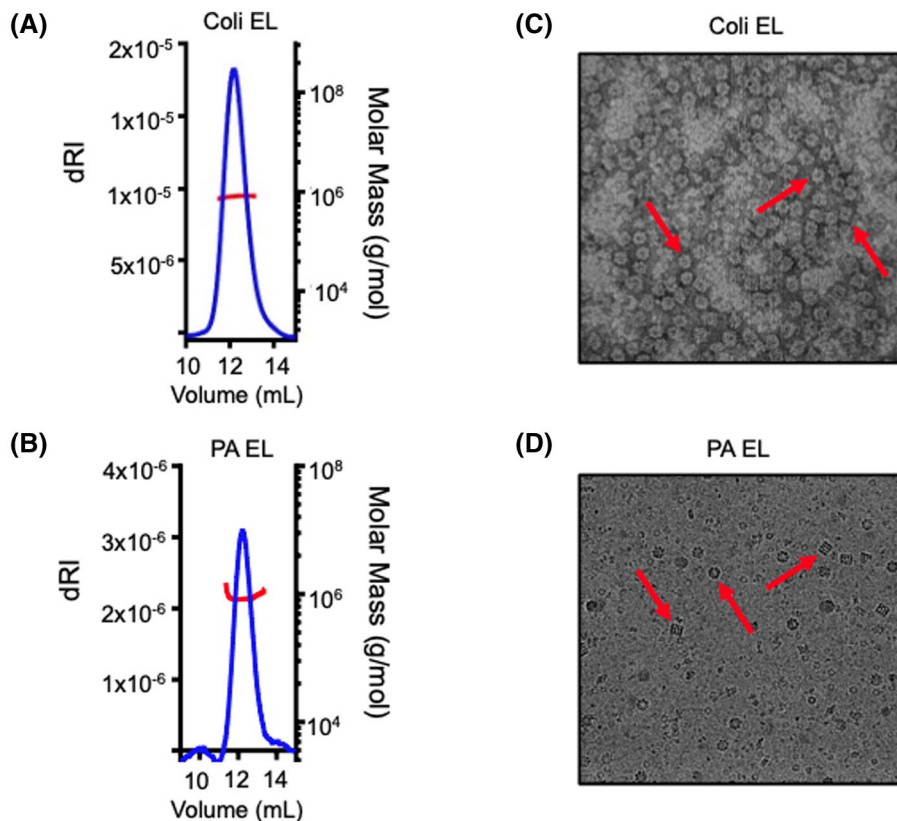


FIGURE 3 Purified GroEL has a tetradecameric structure. (A) GroEL^{coli} SEC-MALS and (B) GroEL^{P. aeruginosa} SEC-MALS indicate 800 kDa predicted mass. (C,D) Electron micrographs of GroEL^{coli} and GroEL^{P. aeruginosa}, respectively. Red pointer indicates an example of tetradecameric GroEL (side and top views)

lose contact with one another first, followed by depolymerization of each ring (Figures S4 and S5).

3.2 | ATP-dependent positive and negative allostery differs between GroEL^{coli}, GroEL^{ESKAPE}, and GroEL^{chimera}

We wished to characterize differences in the heterooligomeric GroEL, GroEL^{chimera} (made up of monomers with variations of ESKAPE and *E. coli* GroEL domains), and GroEL^{ESKAPE} to determine how they operate and how the expression of these chaperones affects cell viability. Although each of the GroEL^{ESKAPE} can support organism viability (with exception of GroEL^{S. aureus}), all GroEL^{ESKAPE} differ from GroEL^{coli} by V_{max} , K_m , allosteric transition states, and/or intra-ring coupling free energy (Figure 4A,B, and Table 1). Interestingly, when GroEL^{ESKAPE} is co-expressed in *E. coli* with GroEL^{coli}, colony phenotypes matching that of the parent *E. coli* strain itself were noted with *groESL*^{A. baumannii} expression only (not shown). Replacement of *E. coli groESL*^{coli} with *groESL*^{A. baumannii} was also the only knock-in strain which

did not display an abnormal planktonic phenotype at any temperature.²⁵ We found no statistical difference between GroEL^{coli} and GroEL^{A. baumannii} regarding K_m , K_{cat}/K_m , ATP concentration for the first allosteric transition from tense to relaxed state (positive allostery between subunits within same GroEL ring), Hill coefficient for positive allostery (cooperativity), and Hill coefficient for negative allostery (cooperativity) (Figure 4A,B and Table 1). GroEL^{K. pneumoniae} and GroEL^{E. cloacae}, which rescue LG6, but display abnormal phenotypes in their respective *E. coli* knock-in strains,²⁵ were found to have similar K_{cat}/K_m and positive allostery Hill slope values compared to GroEL^{coli}. GroEL^{E. faecium} and GroEL^{P. aeruginosa}, which form nonfunctional GroEL heterooligomers when co-expressed with GroEL^{coli}, differ from GroEL^{coli} when comparing K_m , first transition point, and second transition points (negative allostery between GroEL rings transitioning from tense to relaxed state).

Although GroEL^{coli} and GroEL^{P. aeruginosa} are active when expressed and purified as homotetradecameric chaperonins, heterooligomeric chaperonins containing monomers from each species were found to be inactive when co-expressed and purified in *E. coli*.²⁵ To investigate which GroEL domain may be responsible for the loss

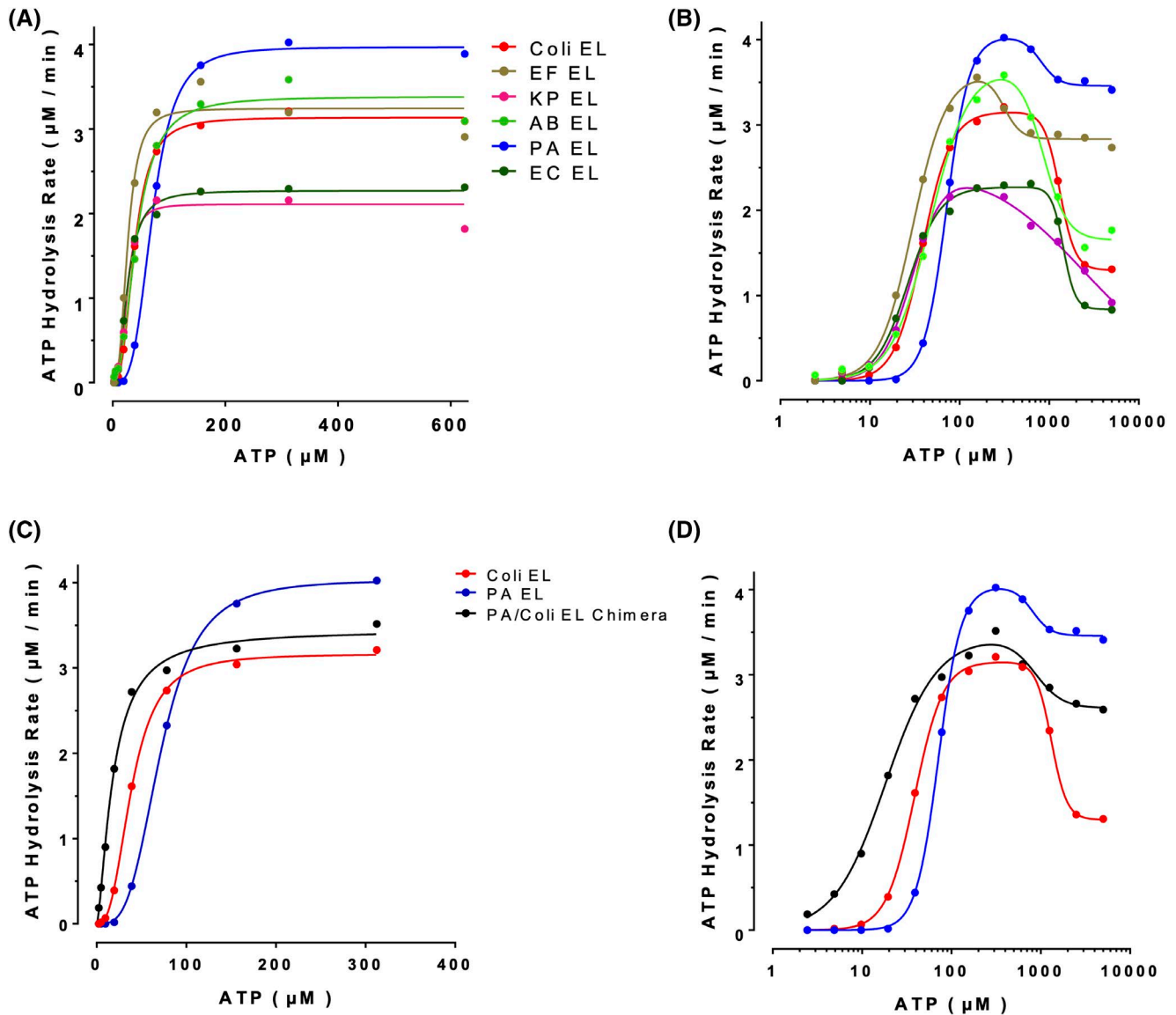


FIGURE 4 ATP-dependent positive and negative allosteric transitions differ between GroEL^{Coli}, GroEL^{ESKAPE}, and GroEL^{chimera}. (A) ATP hydrolysis rate on a linear scale and (B) log-linear ATP hydrolysis rates for GroEL^{Coli} and GroEL^{ESKAPE} at various ATP concentrations. (C,D) Similarly as above, comparing GroEL^{chimera} (*E. coli* equatorial domain, *P. aeruginosa* apical and intermediate domains) with GroEL^{Coli} and GroEL^{P.aeruginosa}. *E. coli* GroEL (Coli EL), *E. faecium* GroEL (EF EL), *K. pneumoniae* GroEL (KP EL), *A. baumannii* GroEL (AB EL), *P. aeruginosa* GroEL (PA EL), *E. cloacae* GroEL (EC EL). Average values of initial ATPase rates shown from experiments conducted in at least triplicate at 24°C

of GroEL^{P.aeruginosa/coli} heterooligomer activity, chimeric GroEL (GroEL^{chimera}) were generated. Swapping the GroEL^{P.aeruginosa} equatorial domain for GroEL^{Coli} equatorial domain (while maintaining GroEL^{P.aeruginosa} apical and intermediate domains) and expressing this GroEL^{chimera} in LG6 supported cell viability, whereas swapping the apical or intermediate domains did not rescue LG6. Neither combination above for GroEL^{chimera} containing *E. faecium* domains was able to support LG6 viability and was not further studied here.²⁵

There was no statistically significant difference in V_{max} values for GroEL^{chimera} and GroEL^{Coli}, however,

GroEL^{chimera} demonstrated an increased affinity for ATP (Figure 4C,D and Table 1), allosteric transitions at lower ATP concentration (within and between GroEL rings, Figure 4C,D), and decreased positive and negative cooperativity (Table 1). This intermediate phenotype perhaps has intra- and inter-ring cooperativity compatible with GroEL^{Coli} sufficient to refold essential clients for maintenance of cell viability. GroEL^{P.aeruginosa/coli} (as well as GroEL^{E. faecium/coli}) heterooligomers captured by pull-down were devoid of ATPase activity, and therefore cooperativity measurements at various ATP concentrations could not be measured.

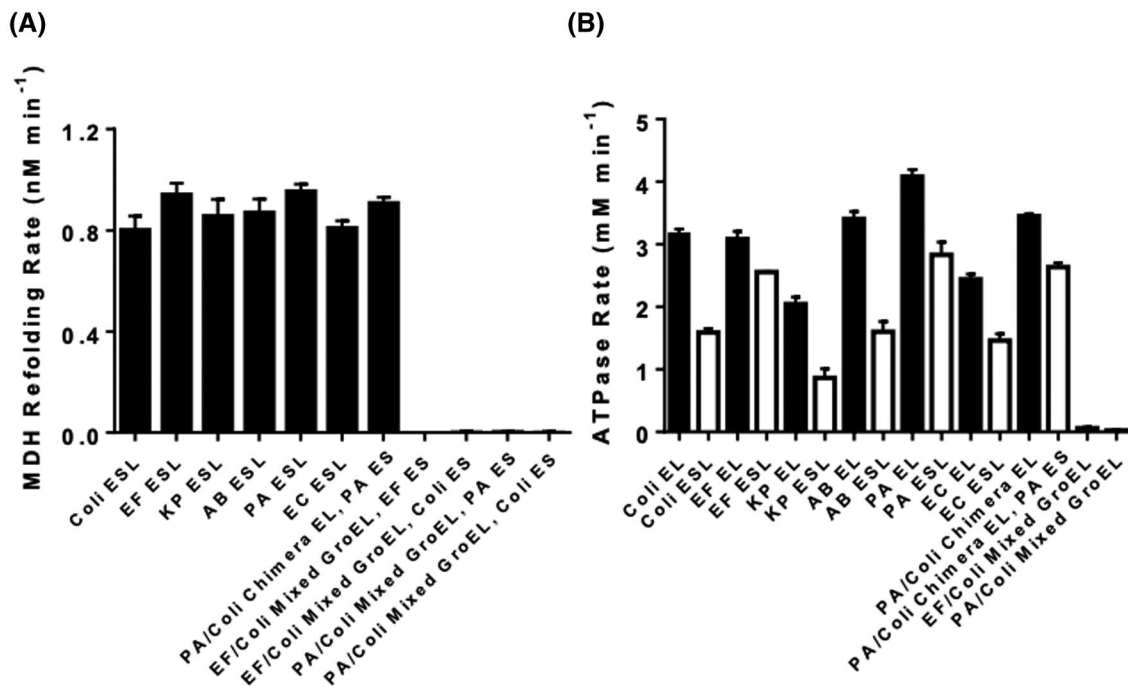


FIGURE 5 GroESL^{ESKAPE} and GroESL^{chimera} refold client polypeptide and demonstrate ATPase activity. (A) GroESL^{coli}, GroESL^{ESKAPE}, and GroESL^{chimera} refold dMDH at a similar rate, whereas heterooligomeric GroEL with GroES is inactive in the refolding assay at 37°C. (B) GroEL (black bars) and GroESL (white bars) ATPase (312.5 μ M ATP) rates for *E. coli*, ESKAPE, chimeric, and heterooligomeric GroELs at 24°C. *E. coli* (Coli), *E. faecium* (EF), *K. pneumoniae* (KP), *A. baumannii* (AB), *P. aeruginosa* (PA), *E. cloacae* (EC)

3.3 | GroESL^{ESKAPE} and GroESL^{chimera} refold client polypeptide and demonstrate ATPase activity comparable to GroESL^{coli}

GroEL^{coli}, GroEL^{ESKAPE}, and GroEL^{chimera} exhibit ATPase rate depression in the presence of their respective GroES and assist in the refolding of denatured malate dehydrogenase (dMDH), a GroESL client (Figure 5). Despite differences in V_{max} , K_m , and positive/negative cooperativity of ATPase activity, GroESL^{ESKAPE} and GroESL^{chimera} refold dMDH at a similar rate compared to GroESL^{coli} (Figure 5A). The dMDH refolding rates for GroEL^{*E. faecium*/coli} and GroEL^{*P. aeruginosa*/coli} heterooligomers were similar to spontaneous refolding when paired with either GroES^{coli} or respective GroES^{ESKAPE}. All GroEL^{ESKAPE}, GroEL^{coli}, and GroEL^{chimera} investigated exhibit ATPase activity; however, heterooligomeric GroEL^{*E. faecium*/coli} and GroEL^{*P. aeruginosa*/coli} (both unable to refold denatured client protein) do not appear to hydrolyze ATP to any appreciable extent (Figure 5B). The addition of species matched GroES (e.g., GroES^{coli} with GroEL^{coli} or GroES^{*E. faecium*} with GroEL^{*E. faecium*}) to each ATPase active GroEL resulted in ATPase rate depression. The extent of ATPase rate depression with species matched GroES and GroEL for GroESL^{*P. aeruginosa*}, GroESL^{*E. faecium*}, and GroESL^{chimera} was less pronounced than the rest of the GroESL tested and may indicate a difference in refolding cycle duration or GroES/GroEL interaction.

3.4 | GroES/GroEL mismatch impedes dMDH refolding rate due to suboptimal GroES/GroEL interaction

Based upon the inability of GroESL^{ESKAPE} to rescue LG6 (GroESL^{coli} deficient) and AI90 (*groES*^{coli} present, *groE-L*^{coli} null) *E. coli* strains in some cases,²⁵ we explored GroES-GroEL incompatibilities as another potential explanation. Using a dMDH refolding assay as a surrogate for global chaperonin-client refolding potential, it was found that when GroES^{coli} was paired with GroEL^{ESKAPE}, this mismatch resulted in a significantly diminished refolding rate when compared to matched GroES^{ESKAPE} and GroEL^{ESKAPE} (with exception of *E. coli* and *E. cloacae* pairings as they have nearly identical amino acid overlap) (Figures 6A and 7A). dMDH refolding rate experiments revealed that conversely paired (GroEL^{coli} paired with GroES^{ESKAPE}) suffered as above, again with exception to *E. coli* and *E. cloacae* pairings (Figure 6B). It was also found that the extent of ATPase rate depression was lessened with GroEL^{coli} paired with GroES^{*E. faecium*}, GroES^{*K. pneumoniae*}, GroES^{*A. baumannii*}, and GroES^{*P. aeruginosa*} (Figure 6C), a potential indicator of impaired GroES/GroEL interaction. We hypothesized this interaction was impaired due to suboptimal interaction between GroES^{ESKAPE} and GroEL^{coli} (or conversely GroES^{coli} and GroEL^{ESKAPE}).

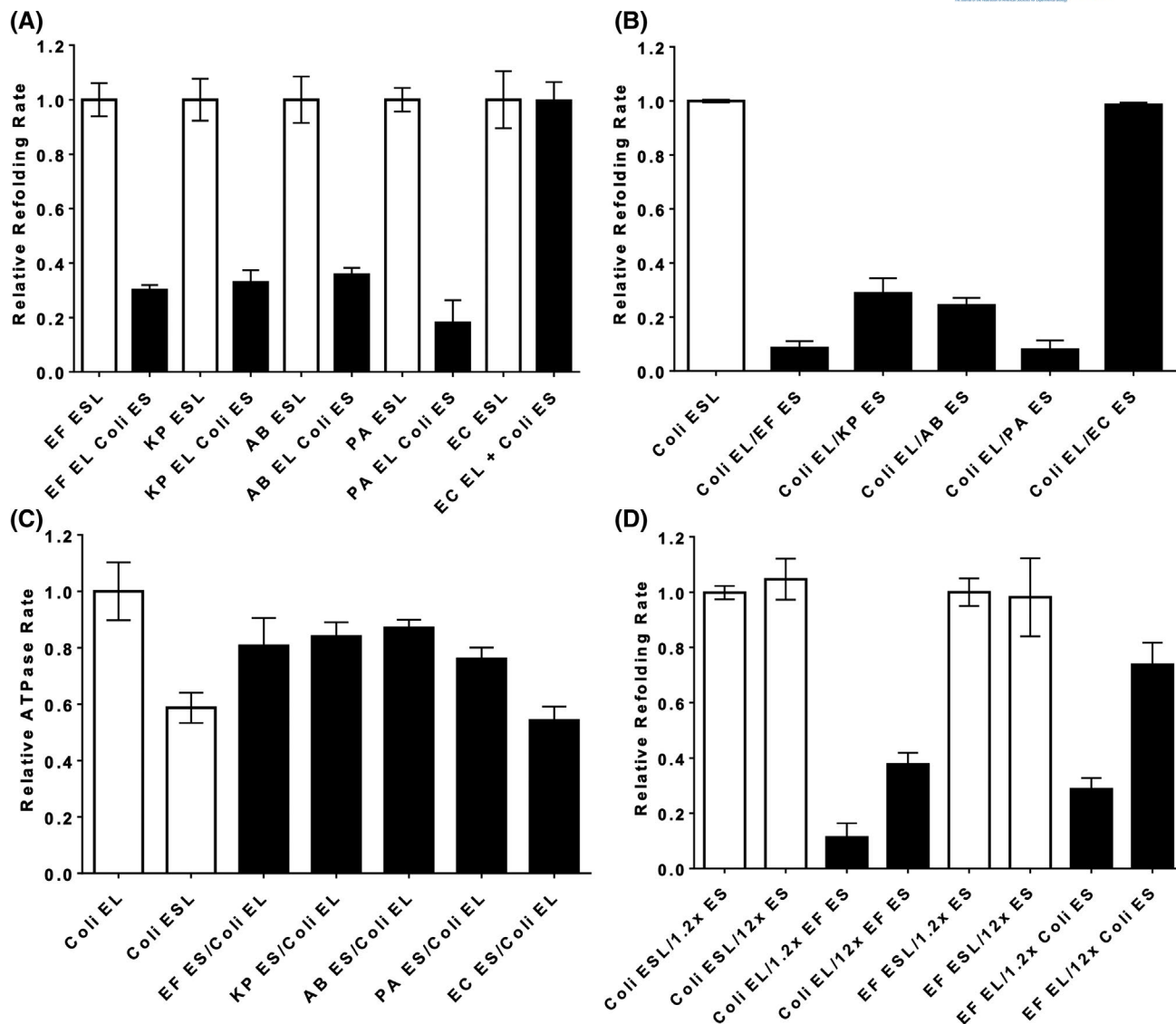


FIGURE 6 GroES/GroEL mismatch impedes dMDH refolding rate due to suboptimal GroES/GroEL interaction. (A) Normalized GroESL^{ESKAPE} (white) refolding rates were compared with mismatched GroEL^{ESKAPE} and GroES^{coli} (black). (B) Normalized GroESL^{coli} (white) refolding rates were compared with mismatched GroEL^{coli} and GroES^{ESKAPE} (black). (C) Normalized GroEL^{coli} ATPase rate (312.5 μ M ATP) at 24°C and GroESL^{coli} (white) ATPase rate compared with GroEL^{coli} and GroES^{ESKAPE} (black) ATPase rates. (D) Normalized GroESL^{coli} and GroESL^{E. faecium} (white) refolding rates compared to mismatched (black) GroEL^{coli}/GroES^{E. faecium} or GroEL^{E. faecium}/GroES^{coli} at 1.2 or 12 fold greater GroES:GroEL. All refolding experiments were done at 37°C. *E. coli* (Coli), *E. faecium* (EF), *K. pneumoniae* (KP), *A. baumannii* (AB), *P. aeruginosa* (PA), *E. cloacae* (EC)

To determine if this phenomenon could be due to a perturbed protein–protein interaction (GroES/GroEL), we repeated the refolding assay with GroESL^{coli}, GroESL^{E. faecium}, or a mismatch between *E. coli* and *E. faecium* GroES and GroEL (GroES^{coli} and GroEL^{E. faecium} or GroES^{E. faecium} and GroEL^{coli}) at 1.2:1 (standard conditions) and 12:1 GroES:GroEL (saturating conditions) (Figure 6D). For *E. coli* and *E. faecium* matched GroES–GroEL refolding (GroESL^{coli} or GroESL^{E. faecium}) combinations, increasing the GroES concentration 10-fold did not increase refolding rate. For mismatched *E. coli* and *E. faecium* GroES–GroEL (GroES^{coli} and GroEL^{E. faecium} or GroES^{E. faecium} and GroEL^{coli}), it was found

that increasing the GroES concentration resulted in an enhanced refolding rate, indicating the mismatched pair may indeed suffer from a perturbed protein–protein interaction, perhaps due to differences in the GroES mobile loop^{10,53} and mobile loop hinge/pivot residues⁵⁴ (Figure 7B,C).

4 | DISCUSSION

In these studies, we investigated the GroEL^{ESKAPE} chaperonins and their cochaperonins. To ensure purity, each chaperonin or cochaperonin was expressed and purified

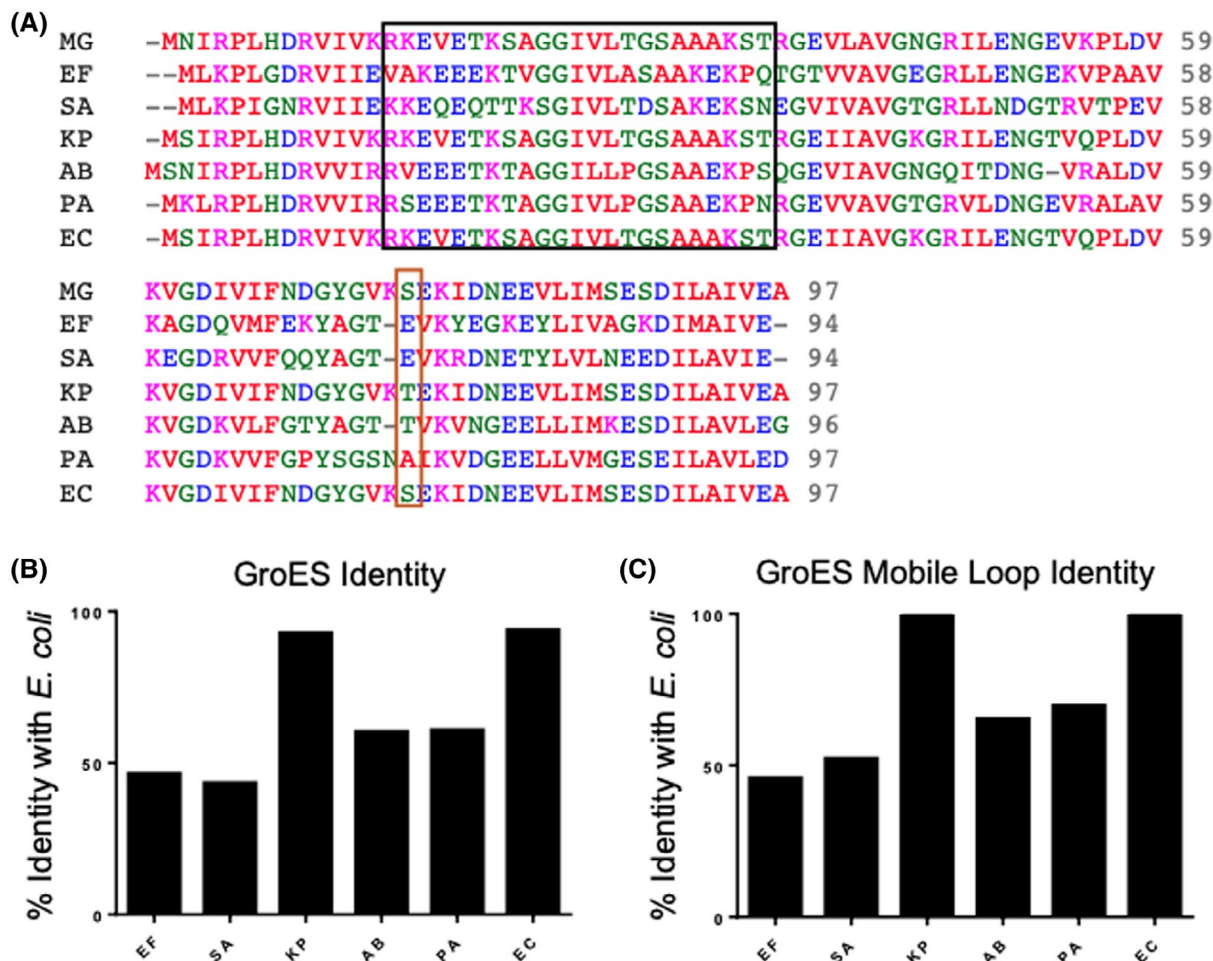


FIGURE 7 Differences in GroES^{ESKAPE} mobile loop and mobile loop hinge region may be responsible for perturbed GroES interaction with GroEL^{coli}. (A) GroES^{ESKAPE} and GroES^{coli} alignment using Clustal Omega with mobile loop (black) and mobile loop hinge region (orange) outlined. *E. coli* (Coli), *E. faecium* (EF), *K. pneumoniae* (KP), *A. baumannii* (AB), *P. aeruginosa* (PA), *E. cloacae* (EC). (B) GroES amino acid identity of ESKAPE pathogens compared to *E. coli*. (C) GroES mobile loop amino acid identity of ESKAPE pathogens compared to *E. coli*

from an *E. coli* knock-in/knock-out strain (where *groESL*^{coli} was replaced by the respective *groESL*^{ESKAPE}). The purity of each of the chaperonins was essential to characterize intra-ring and inter-ring cooperativity and denatured client refolding rate determination. Furthermore, the above rates and cooperativity were compared to functional chimeric and nonfunctional heterooligomeric GroELs. These data explain the phenomena observed in recently reported *E. coli* rescue experiments²⁵ and guide our understanding of the biochemical similarities and differences between ESKAPE and *E. coli* GroESL. Swiss Model homology modeling and AlphaFold models predicted that GroEL^{ESKAPE} would closely resemble GroEL^{coli} monomer structure (Figures S1–S3). Herein, conserved homotetradameric quaternary structure was observed by SEC-MALS, native MS, CD-MS, and electron microscopy (Figures 3, S4, and S5). These predictions, however, fail to explain how the expression of some GroESL^{ESKAPE} is lethal to

GroEL-deficient LG6 or AI90 *E. coli* strains. Due to monomeric translation of GroEL subunits, co-expression of GroEL monomers from different species within the same strain generates mature tetradecamers comprised of both species of GroEL monomers (Figure 1).^{25,55–58}

Heterooligomeric GroEL, made up of GroEL^{K. pneumoniae/coli}, GroEL^{A. baumannii/coli}, or GroEL^{E. cloacae/coli} (but not GroEL^{P. aeruginosa/coli}, GroEL^{E. faecium/coli}, or GroEL^{S. aureus/coli}), were able to rescue the LG6 *E. coli* strain (Table 1). A pull-down experiment of heterooligomeric GroEL^{P. aeruginosa/coli} revealed a fully assembled tetradecamer, devoid of ATPase and refolding activity. Table 1 and Figure 4 outline the differences in GroEL^{coli} and GroEL^{P. aeruginosa} V_{max} and positive and negative allosteric transition points. We hypothesize the observed mismatch in positive and negative allostery for GroEL^{coli} vs. GroEL^{P. aeruginosa} (Figure 4) prevent coordinated ATP hydrolysis (incompatible with organism viability) and thus perturbed cooperativity when

both GroEL species reside within one tetradecameric unit. This allosteric disturbance, in the case of inactive heterooligomeric GroEL, may result from loss of ATP binding to the cis ring, preventing GroES binding, leading to loss of client polypeptide refolding. Alternatively, perturbed negative allostery⁵⁹ may prevent the ATP binding event in the trans ring from generating sufficient force to eject GroES and ADP from the cis ring, resulting in an SR1 (single ring)-like^{27,43} single turnover event which traps protein client and prevents further client refolding. At high temperatures, GroEL loses its negative allostery and traps any internalized protein.⁶⁰ Client refolding proceeds normally below heat shock temperatures, but at heat shock temperatures, GroEL negative allostery is lost (absent ring-ring communication and refolding function until lower temperatures obtain). Although several of the GroEL^{ESKAPE} appear to have less pronounced negative allostery compared to GroEL^{coli} at 24°C (Figure 4), refolding experiments up to 37°C did not result in the compromised refolding activity of any GroEL^{ESKAPE} when paired with their native GroES. However, observed from purposely generated heterooligomeric GroEL^{coli} (containing varied numbers of wild-type and mutant GroEL^{coli} monomers within a GroEL tetradecamer) was that the introduction of a single mutant monomer into wild-type GroEL tetradecamer can hinder chaperone activity.^{20,40,43} Within LG6, sufficient endogenous chaperonin was expressed even during glucose suppression of the chromosomal lac-promoted *groESL*^{coli} (with simultaneous induction of plasmid-borne ESKAPE *groESL*) in which dominant-negative heterooligomeric GroEL were generated (Table 1).²⁵ From our previous work,²⁵ *E. coli* containing separate plasmids with different expression systems (*P_{BAD}* or *lac*) encoding different *groEL* genes (*groEL*^{coli} and *groEL*^{*E. faecium*} (or *groEL*^{*P. aeruginosa*})) were chemically induced to generate heterooligomeric GroEL tetradecamers comprised of GroEL^{coli} and GroEL^{*E. faecium*} (or GroEL^{*P. aeruginosa*}). The ratio of monomers incorporated into the heterotetradecameric GroEL was directly proportional to the extent of chemical induction of each plasmid (GroEL monomer abundance tested at 1:3, 1:2, and 1:1 as GroEL^{ESKAPE}:GroEL^{coli}). A careful titration in which heterotetradecamers containing 1 to 13 GroEL^{*E. faecium*} (or GroEL^{*P. aeruginosa*}) were not generated in this study to identify the minimum number of GroEL^{*E. faecium*} (or GroEL^{*P. aeruginosa*}) required to poison the chaperoning ability of heterotetradecameric GroEL also containing GroEL^{coli}.

GroEL^{chimera} was generated to understand which GroEL domain^{26,28} could be responsible for incompatibility regarding lack of ATPase or refolding activity within the GroEL^{*P. aeruginosa/coli*} heterooligomer. Of all chimeras generated,²⁵ only *E. coli* equatorial domain/*P. aeruginosa* intermediate-apical domain GroEL^{chimera} could rescue

LG6. As noted in Figure 4C,D, positive and negative cooperativity were perturbed with this chimera compared to GroEL^{coli} and GroEL^{*P. aeruginosa*}, indicating that the equatorial domains (within the GroEL heterotetradecamer) may be responsible for incompatibility (either through differences in important inter-ring or intra-ring residue contacts).⁴¹ It has been reported previously that a steeper hill slope regarding positive cooperativity was associated with more rapid GroES release.⁴² We hypothesized that the increase in ATP affinity for both first and second allosteric transitions, but a corresponding decrease in subunit cooperativity for GroEL^{chimera}, may be needed to overcome the allosteric mismatch between GroEL^{*P. aeruginosa/coli*} heterooligomers for the appropriate coordination of GroES binding and dissociation. This phenomenon will be further investigated by generating ring mutations to support our hypothesis.

In contrast to GroEL^{*P. aeruginosa*}, GroEL^{*E. faecium*} was only viable when *groESL*^{coli} was removed from the *E. coli* chromosome and replaced by *groESL*^{*E. faecium*}. Purified GroEL^{*E. faecium*} showed perturbed positive and negative allostery compared to GroEL^{coli} (Figure 4) and co-expression with GroEL^{coli} generated an inactive heterooligomer GroEL^{*E. faecium/coli*}. GroEL^{*E. faecium/coli*} chimeras were made, but replacement with both *E. coli* apical and equatorial domains was required (only the GroEL^{*E. faecium*} intermediate domain remained) for the rescue of LG6 *E. coli*. This observation indicates possible positive/negative allosteric differences to GroEL^{coli}, but also possible is GroEL^{*E. faecium*}-GroES^{coli} incompatibilities. As apical domain client polypeptide recognition is of utmost importance in the GroESL refolding cycle,^{29,61-67} we recognize the possibility that heterooligomers containing both GroEL^{*E. faecium/coli*} chimeric subunits and GroEL^{coli} subunits may lack recognition of essential proteins in *E. coli* (and result in lack of cell viability/rescue). GroES or GroES-mimics from other organisms have been shown to interact with GroEL^{coli}.⁶⁸⁻⁷¹ GroESL^{*E. faecium*} could not rescue the AI90 *E. coli* strain (*groES*^{coli} present, *groEL*^{coli} knockout maintained by an inducible plasmid containing *groEL*^{coli}). We do not rule out the possibility of GroES heterooligomer as a cause of loss of cell viability, but we also find the GroEL^{*E. faecium*}-GroES^{coli} pairing severely decreases client refolding rate (Figure 6), indicating a potential suboptimal protein-protein interaction. We do not discount the fact that this explanation may also be contributing to the dominant-negative effect observed in LG6 (in addition to the formation of inactive GroEL heterooligomers). This is supported by studies that have elucidated that proper GroES-GroEL protein-protein interaction was most predictive of refolding rate of client substrate and holds true for mutant GroES^{coli} or GroES (which have inefficient interaction with GroEL) from

other organisms.^{72–75} It is unlikely that the GroES^{coli}-GroEL^{E. faecium} interaction is taking place, but not eliciting proper force to propagate the necessary transmission of signal to eject polypeptide, GroES, and nucleotide from the opposite ring (GroEL trans ring) (Figure 2B, step 5). The highest support for the perturbed GroES/GroEL interaction comes from the fact that this suboptimal interaction reduces the time GroES interacts with GroEL and thus disrupts the refolding cycle timing (or is less likely to initiate the refolding cycle), ultimately leading to less efficient client refolding^{72–74} (Figure 6A,B). Additionally, altered refolding cycle timing is supported by our ATPase rate measurements (diminished GroES interaction with GroEL effectively contributes to reduced ATPase rate depression) (Figure 6C).

Overall, noted in this work is predicted structural similarity between GroEL^{ESKAPE} and GroEL^{coli} with differences in intra- and inter-ring cooperativity. These differences are magnified during co-expression which generates heterooligomeric GroEL, resulting in *E. coli* planktonic phenotypes including nonviable, viable with elongation at high or low temperature, or viable without visible defects. These phenotypes seem to be directly correlated with the conservation of positive and negative cooperativity for GroEL^{ESKAPE} to that of GroEL^{coli}. In the presence of functional GroEL, we have also shown that GroES-GroEL mismatch (which may be the cause of lack of rescue in the case of AI90 or possibly even LG6 *E. coli* strains) decreased the rate at which model substrate dMDH refolding occurred and may contribute to altered organism phenotype or non-viability. Untested was the substrate scope of each GroESL^{ESKAPE} to determine if differences in intrinsic client recognition, duration of refolding cycle, or residue exposure within GroEL contributed to perturbed phenotype for the *groESL*^{ESKAPE} knock-in *E. coli* and is something we will follow up with as a future direction. To understand the allosteric differences in GroEL^{ESKAPE} compared to GroEL^{coli}, the structures of each GroEL^{ESKAPE} will be solved by cryo-electron microscopy. These data can be used to determine at the amino acid level if key salt bridges or other interactions are known to be of importance in GroEL^{coli} allostery are indeed altered in GroEL^{ESKAPE}. In all, the data presented in this work provide a better understanding of the GroESL^{ESKAPE} chaperone systems and prepare for a push toward developing antimicrobials that target mechanisms of chaperonin allostery.

ACKNOWLEDGMENTS

The authors would like to acknowledge Arthur L. Horwich and Peter Lund for supplying the LG-6 and AI90 strains.

DISCLOSURES

S.M.J. and E.C. are cofounders of BioEL, Inc.

AUTHOR CONTRIBUTIONS

Conceptualization: Jared Sivinski and Eli Chapman. *Methodology:* Jared Sivinski, Duc Ngo, Marius M. Kostelic, Chunxiang Wu, Michael T. Marty, Edmond R. Watson; *Validation,* Jared Sivinski, Duc Ngo, Christopher J. Zerio, Andrew J. Ambrose, Edmond R. Watson, Lynn K. Kaneko, Marius M. Kostelic, Mckayla Stevens, Anne-Marie Ray, Yangshin Park, Chunxiang Wu, Michael T. Marty, Quyen Q. Hoang, Gabriel C. Lander, Steven M. Johnson, and Eli Chapman. *Investigation:* Jared Sivinski, Duc Ngo, Christopher J. Zerio, Andrew J. Ambrose, Edmond R. Watson, Lynn K. Kaneko, Marius M. Kostelic, Mckayla Stevens, Anne-Marie Ray, Yangshin Park, and Chunxiang Wu. *Writing—Original Draft:* Jared Sivinski. *Writing—Review & Editing:* Jared Sivinski, Duc Ngo, Christopher J. Zerio, Andrew J. Ambrose, Edmond R. Watson, Lynn K. Kaneko, Marius M. Kostelic, Mckayla Stevens, Anne-Marie Ray, Yangshin Park, Chunxiang Wu, Michael T. Marty, Quyen Q. Hoang, Gabriel C. Lander, Steven M. Johnson, and Eli Chapman. *Funding Acquisition:* Jared Sivinski, Edmond R. Watson, Michael T. Marty, Quyen Q. Hoang, Donna D. Zhang, Gabriel C. Lander, Steven M. Johnson, and Eli Chapman. *Resources:* Michael T. Marty, Quyen Q. Hoang, Donna D. Zhang, Gabriel C. Lander, Steven M. Johnson, and Eli Chapman. *Supervision:* Michael T. Marty, Quyen Q. Hoang, Donna D. Zhang, Gabriel C. Lander, Steven M. Johnson, and Eli Chapman.

DATA AVAILABILITY STATEMENT

All data generated for this submission is contained within the manuscript.

ORCID

Jared Sivinski  <https://orcid.org/0000-0003-2696-6279>

Steven M. Johnson  <https://orcid.org/0000-0001-7254-4128>

REFERENCES

1. Clatworthy AE, Pierson E, Hung DT. Targeting virulence: a new paradigm for antimicrobial therapy. *Nat Chem Biol.* 2007;3(9):541-548.
2. Santajit S, Indrawattana N. Mechanisms of antimicrobial resistance in ESKAPE pathogens. *Biomed Res Int.* 2016;2016:2475067.
3. Braig K, Otwinowski, Z, Hegde, R, et al. The crystal structure of the bacterial chaperonin GroEL at 2.8 Å. *Nature.* 1994;371(6498):578-586.
4. Chapman E, Farr GW, Usaite R, et al. Global aggregation of newly translated proteins in an *Escherichia coli* strain deficient of the chaperonin GroEL. *Proc Natl Acad Sci U S A.* 2006;103(43):15800-15805.

5. Fayet O, Ziegelhoffer T, Georgopoulos C. The groES and groEL heat shock gene products of *Escherichia coli* are essential for bacterial growth at all temperatures. *J Bacteriol.* 1989;171(3):1379-1385.
6. Horwich AL, Willison KR. Protein folding in the cell: functions of two families of molecular chaperone, hsp 60 and TF55-TCPI. *Philos Trans R Soc Lond B Biol Sci.* 1993;339(1289):313-325; discussion 325-326.
7. Van Dyk TK, Gatenby AA, LaRossa RA. Demonstration by genetic suppression of interaction of GroE products with many proteins. *Nature.* 1989;342(6248):451-453.
8. Georgescauld F, Popova K, Gupta A, et al. GroEL/ES chaperonin modulates the mechanism and accelerates the rate of TIM-barrel domain folding. *Cell.* 2014;157(4):922-934.
9. Ma J, Karplus M. The allosteric mechanism of the chaperonin GroEL: a dynamic analysis. *Proc Natl Acad Sci U S A.* 1998;95(15):8502-8507.
10. Xu Z, Horwich AL, Sigler PB. The crystal structure of the asymmetric GroEL-GroES-(ADP)₇ chaperonin complex. *Nature.* 1997;388(6644):741-750.
11. Zahn R, Buckle AM, Perrett S, et al. Chaperone activity and structure of monomeric polypeptide binding domains of GroEL. *Proc Natl Acad Sci U S A.* 1996;93(26):15024-15029.
12. Ivic A, Olden D, Wallington EJ, Lund PA. Deletion of *Escherichia coli* groEL is complemented by a *Rhizobium leguminosarum* groEL homologue at 37 degrees C but not at 43 degrees C. *Gene.* 1997;194(1):1-8.
13. Abdeen S, Kunkle T, Salim N, et al. Sulfonamido-2-arylbenzoxazole GroEL/ES inhibitors as potent antibacterials against methicillin-resistant *Staphylococcus aureus* (MRSA). *J Med Chem.* 2018;61(16):7345-7357.
14. Abdeen S, Salim N, Mammadova N, et al. GroEL/ES inhibitors as potential antibiotics. *Bioorg Med Chem Lett.* 2016;26(13):3127-3134.
15. Kunkle T, Abdeen S, Salim N, et al. Hydroxybiphenylamide GroEL/ES inhibitors are potent antibacterials against planktonic and biofilm forms of *Staphylococcus aureus*. *J Med Chem.* 2018;61(23):10651-10664.
16. Chaudhuri RR, Allen AG, Owen P, et al. Comprehensive identification of essential *Staphylococcus aureus* genes using transposon-mediated differential hybridisation (TMDH). *BMC Genom.* 2009;10:29.
17. Gallagher LA, Ramage E, Weiss EJ, et al. Resources for genetic and genomic analysis of emerging pathogen *Acinetobacter baumannii*. *J Bacteriol.* 2015;197(12):2027-2035.
18. Lewin GR, Stacy A, Michie KL, et al. Large-scale identification of pathogen essential genes during coinfection with sympatric and allopatric microbes. *Proc Natl Acad Sci U S A.* 2019;116(39):19685-19694.
19. Mulani MS, Kamble EE, Kumkar SN, Tawre MS, Pardesi KR. Emerging strategies to combat ESKAPE pathogens in the era of antimicrobial resistance: a review. *Front Microbiol.* 2019;10(539):1-24.
20. Persyn E, Sassi M, Aubry M, et al. Rapid genetic and phenotypic changes in *Pseudomonas aeruginosa* clinical strains during ventilator-associated pneumonia. *Sci Rep.* 2019;9(4720):1-8.
21. Ramage B, Erolin R, Held K, et al. Comprehensive arrayed transposon mutant library of klebsiella pneumoniae outbreak strain KPN1H1. *J Bacteriol.* 2017;199(20):1-9.
22. Shah R, Large AT, Ursinus A, et al. Replacement of GroEL in *Escherichia coli* by the Group II chaperonin from the archaeon *Methanococcus maripaludis*. *J Bacteriol.* 2016;198(19):2692-2700.
23. Chilukoti N, Kumar CM, Mande SC. GroEL2 of *Mycobacterium tuberculosis* reveals the importance of structural pliability in chaperonin function. *J Bacteriol.* 2016;198(3):486-497.
24. Kumar CMS, Khare G, Srikanth CV, et al. Facilitated oligomerization of mycobacterial GroEL: evidence for phosphorylation-mediated oligomerization. *J Bacteriol.* 2009;191(21):6525-6538.
25. Sivinski J, Ambrose AJ, Panfilenko I, et al. Functional differences between *E. coli* and ESKAPE pathogen GroES/GroEL. *MBio.* 2021;12(1).
26. Bukau B, Horwich AL. The Hsp70 and Hsp60 chaperone machines. *Cell.* 1998;92(3):351-366.
27. Hayer-Hartl MK, Weber F, Hartl FU. Mechanism of chaperonin action: GroES binding and release can drive GroEL-mediated protein folding in the absence of ATP hydrolysis. *EMBO J.* 1996;15(22):6111-6121.
28. Lorimer GH. GroEL structure: a new chapter on assisted folding. *Structure.* 1994;2(12):1125-1128.
29. Weaver J, Jiang M, Roth A, Puchalla J, Zhang J, Rye HS. GroEL actively stimulates folding of the endogenous substrate protein PepQ. *Nat Commun.* 2017;8:15934.
30. Koshland DE Jr, Nemethy G, Filmer D. Comparison of experimental binding data and theoretical models in proteins containing subunits. *Biochemistry.* 1966;5(1):365-385.
31. Monod J, Wyman J, Changeux JP. On the nature of allosteric transitions: a plausible model. *J Mol Biol.* 1965;12:88-118.
32. Yifrach O, Horovitz A. Two lines of allosteric communication in the oligomeric chaperonin GroEL are revealed by the single mutation Arg196→Ala. *J Mol Biol.* 1994;243(3):397-401.
33. Yifrach O, Horovitz A. Nested cooperativity in the ATPase activity of the oligomeric chaperonin GroEL. *Biochemistry.* 1995;34(16):5303-5308.
34. Horovitz A. The relation between cooperativity in ligand binding and intramolecular cooperativity in allosteric proteins. *Proc R Soc Lond.* 1995;259:85-87.
35. Danziger O, Rivenzon-Segal D, Wolf SG, Horovitz A. Conversion of the allosteric transition of GroEL from concerted to sequential by the single mutation Asp-155 → Ala. *Proc Natl Acad Sci U S A.* 2003;100(24):13797-13802.
36. Horovitz A, Willison KR. Allosteric regulation of chaperonins. *Curr Opin Struct Biol.* 2005;15(6):646-651.
37. Grallert H, Buchner J. Review: a structural view of the GroE chaperone cycle. *J Struct Biol.* 2001;135(2):95-103.
38. Koike-Takeshita A, Yoshida M, Taguchi H. Revisiting the GroEL-GroES reaction cycle via the symmetric intermediate implied by novel aspects of the GroEL(D398A) mutant. *J Biol Chem.* 2008;283(35):23774-23781.
39. Taguchi H. Reaction cycle of chaperonin GroEL via symmetric "football" intermediate. *J Mol Biol.* 2015;427(18):2912-2918.
40. Weiss C, Jebara F, Nisemlat S, Azem A. Dynamic complexes in the chaperonin-mediated protein folding cycle. *Front Mol Biosci.* 2016;3(80):1-8.
41. Clare D, Vasishtan D, Stagg S, et al. ATP-triggered conformational changes delineate substrate-binding and -folding mechanics of the GroEL chaperonin. *Cell.* 2012;149(1):113-123.
42. Fridmann Y, Kafri G, Danziger O, et al. Dissociation of the GroEL-GroES asymmetric complex is accelerated by increased cooperativity in ATP binding to the GroEL ring distal to GroES. *Biochemistry.* 2002;41(18):5938-5944.

43. Rye HS, Burston SG, Fenton WA, et al. Distinct actions of cis and trans ATP within the double ring of the chaperonin GroEL. *Nature*. 1997;388(6644):792-798.
44. Datsenko KA, Wanner BL. One-step inactivation of chromosomal genes in *Escherichia coli* K-12 using PCR products. *Proc Natl Acad Sci U S A*. 2000;97(12):6640-6645.
45. Lanzetta PA, Alvarez LJ, Reinach PS, et al. An improved assay for nanomole amounts of inorganic phosphate. *Anal Biochem*. 1979;100(1):95-97.
46. Kostelic MM, Zak CK, Liu Y, et al. UniDecCD: Deconvolution of Charge Detection-Mass Spectrometry Data, Analytical Chemistry. 2021;93(44):14722-14729. <https://doi.org/10.1021/acs.analchem.1c03181>.
47. Marty MT, Baldwin AJ, Marklund EG, et al. Bayesian deconvolution of mass and ion mobility spectra: from binary interactions to polydisperse ensembles. *Anal Chem*. 2015;87(8):4370-4376.
48. Kostelic MM, Ryan AM, Reid DJ, et al. Expanding the types of lipids amenable to native mass spectrometry of lipoprotein complexes. *J Am Soc Mass Spectrom*. 2019;30(8):1416-1425.
49. Marty MT. Eliminating artifacts in electrospray deconvolution with a softmax function. *J Am Soc Mass Spectrom*. 2019;30(10):2174-2177.
50. Scarff CA, Fuller MJG, Thompson RF, et al. Variations on negative stain electron microscopy methods: tools for tackling challenging systems. *J Vis Exp*. 2018;132:1-18.
51. Jumper J, Evans R, Pritzel A, et al. Highly accurate protein structure prediction with AlphaFold. *Nature*. 2021;596(7873):583-589.
52. Varadi M, Anyango S, Deshpande M, et al. AlphaFold protein structure database: massively expanding the structural coverage of protein-sequence space with high-accuracy models. *Nucleic Acids Res*. 2021;50(D1):439-444.
53. Weissman JS, Hohl CM, Kovalenko O, et al. Mechanism of GroEL action: productive release of polypeptide from a sequestered position under GroES. *Cell*. 1995;83(4):577-587.
54. Lu HM, Liang J. Perturbation-based Markovian transmission model for probing allosteric dynamics of large macromolecular assembling: a study of GroEL-GroES. *PLoS Comput Biol*. 2009;5(10):e1000526.
55. Chapman E, Farr GW, Fenton WA, et al. Requirement for binding multiple ATPs to convert a GroEL ring to the folding-active state. *Proc Natl Acad Sci U S A*. 2008;105(49):19205-19210.
56. Gould PS, Burgar HR, Lund PA. Homologous cpn60 genes in *Rhizobium leguminosarum* are not functionally equivalent. *Cell Stress Chaperones*. 2007;12(2):123-131.
57. Motojima F, Chaudhry C, Fenton WA, et al. Substrate polypeptide presents a load on the apical domains of the chaperonin GroEL. *Proc Natl Acad Sci U S A*. 2004;101(42):15005-15012.
58. Shiseki K, Murai N, Motojima F, et al. Synchronized domain-opening motion of GroEL is essential for communication between the two rings. *J Biol Chem*. 2001;276(14):11335-11338.
59. Fridmann Y, Ulitzur S, Horovitz A. In vivo and in vitro function of GroEL mutants with impaired allosteric properties. *J Biol Chem*. 2000;275(48):37951-37956.
60. Llorca O, Galán A, Carrascosa JL, et al. GroEL under heat-shock. Switching from a folding to a storing function. *J Biol Chem*. 1998;273(49):32587-32594.
61. Chen L, Sigler PB. The crystal structure of a GroEL/peptide complex: plasticity as a basis for substrate diversity. *Cell*. 1999;99(7):757-768.
62. Coyle JE, Jaeger J, Groß M, et al. Structural and mechanistic consequences of polypeptide binding by GroEL. *Fold Des*. 1997;2(6):R93-R104.
63. Feltham JL, Gierasch LM. GroEL-substrate interactions: molding the fold, or folding the mold? *Cell*. 2000;100(2):193-196.
64. Kerner MJ, Naylor DJ, Ishihama Y, et al. Proteome-wide analysis of chaperonin-dependent protein folding in *Escherichia coli*. *Cell*. 2005;122(2):209-220.
65. Priya S, Sharma SK, Sood V, et al. GroEL and CCT are catalytic unfoldases mediating out-of-cage polypeptide refolding without ATP. *Proc Natl Acad Sci U S A*. 2013;110(18):7199-7204.
66. Sigler PB, Xu Z, Rye HS, et al. Structure and function in GroEL-mediated protein folding. *Annu Rev Biochem*. 1998;67:581-608.
67. Weissman JS, Rye HS, Fenton WA, et al. Characterization of the active intermediate of a GroEL-GroES-mediated protein folding reaction. *Cell*. 1996;84(3):481-490.
68. van der Vies SM, Gatenby AA, Georgopoulos C. Bacteriophage T4 encodes a co-chaperonin that can substitute for *Escherichia coli* GroES in protein folding. *Nature*. 1994;368(6472):654-656.
69. Richardson A, van der Vies SM, Keppel F, et al. Compensatory changes in GroEL/Gp31 affinity as a mechanism for allele-specific genetic interaction. *J Biol Chem*. 1999;274(1):52-58.
70. Richardson A, Georgopoulos C. Genetic analysis of the bacteriophage T4-encoded cochaperonin Gp31. *Genetics*. 1999;152(4):1449-1457.
71. Georgopoulos CP, Hendrix RW, Casjens SR, et al. Host participation in bacteriophage lambda head assembly. *J Mol Biol*. 1973;76(1):45-60.
72. Liu H, Kovacs E, Lund PA. Characterisation of mutations in GroES that allow GroEL to function as a single ring. *FEBS Lett*. 2009;583(14):2365-2371.
73. Illingworth M, Ramsey A, Zheng Z, et al. Stimulating the substrate folding activity of a single ring GroEL variant by modulating the cochaperonin GroES. *J Biol Chem*. 2011;286(35):30401-30408.
74. Illingworth M, Ellis H, Chen L. Creating the functional single-ring GroEL-GroES chaperonin systems via modulating GroEL-GroES interaction. *Sci Rep*. 2017;7(1):9710.
75. Figueiredo L, Klunker D, Ang D, et al. Functional characterization of an archaeal GroEL/GroES chaperonin system: significance of substrate encapsulation. *J Biol Chem*. 2004;279(2):1090-1099.

SUPPORTING INFORMATION

Additional supporting information may be found in the online version of the article at the publisher's website.

How to cite this article: Sivinski J, Ngo D, Zerio CJ, et al. Allosteric differences dictate GroEL complementation of *E. coli*. *FASEB J*. 2022;36:e22198. doi:[10.1096/fj.202101708RR](https://doi.org/10.1096/fj.202101708RR)